



## Effects of substrate bias voltage and target sputtering power on the structural and tribological properties of carbon nitride coatings



Pengfei Wang<sup>a,b,\*</sup>, Takanori Takeno<sup>c</sup>, Julien Fontaine<sup>d</sup>, Masami Aono<sup>e</sup>, Koshi Adachi<sup>c</sup>, Hiroyuki Miki<sup>f</sup>, Toshiyuki Takagi<sup>b</sup>

<sup>a</sup> Institute of Nanosurface Science and Engineering, College of Mechatronics and Control Engineering, Shenzhen University, Shenzhen 518060, China

<sup>b</sup> Institute of Fluid Science, Tohoku University, Katahira 2-1-1, Aoba-ku, Sendai 980-8577, Japan

<sup>c</sup> Laboratory of Nanointerface Engineering, Division of Mechanical Engineering, Tohoku University, Aoba 6-6-1, Aramaki, Aoba-ku, Sendai 980-8579, Japan

<sup>d</sup> Laboratoire de Tribologie et Dynamique des Systèmes, UMR 5513 – CNRS/Ecole Centrale de Lyon, Bâtiment H10, 36 Avenue Guy de Collongue, 69134 Écully Cedex, France

<sup>e</sup> Department of Materials Science and Engineering, National Defense Academy, 1-10-20 Hashirimizu, Yokosuka, Kanagawa 239-8686, Japan

<sup>f</sup> Center for Interdisciplinary Research, Tohoku University, Aoba 6-3, Aramaki, Aoba-ku, Sendai 980-8578, Japan

### H I G H L I G H T S

- Various CN<sub>x</sub> coatings are produced using a unique hybrid coating process.
- Structural and tribological properties of CN<sub>x</sub> coatings are investigated.
- The lowest friction coefficient of 0.12 is achieved at –800 V 100 W.
- Friction is controlled by the directly sliding between coating and steel pin.
- Friction reduction is due to decrease of sp<sup>3</sup> carbon bonding in the coating.

### A R T I C L E I N F O

#### Article history:

Received 25 October 2013

Received in revised form

20 January 2014

Accepted 17 February 2014

#### Keywords:

Coatings

Microstructure

Hardness

Friction

### A B S T R A C T

Effects of substrate bias voltage and target sputtering power on the structural and tribological properties of carbon nitride (CN<sub>x</sub>) coatings are investigated. CN<sub>x</sub> coatings are fabricated by a hybrid coating process with the combination of radio frequency plasma enhanced chemical vapor deposition (RF PECVD) and DC magnetron sputtering at various substrate bias voltage and target sputtering power in the order of –400 V 200 W, –400 V 100 W, –800 V 200 W, and –800 V 100 W. The deposition rate, N/C atomic ratio, and hardness of CN<sub>x</sub> coatings as well as friction coefficient of CN<sub>x</sub> coating sliding against AISI 52100 pin in N<sub>2</sub> gas stream decrease, while the residual stress of CN<sub>x</sub> coatings increases with the increase of substrate bias voltage and the decrease of target sputtering power. The highest hardness measured under single stiffness mode of 15.0 GPa and lowest residual stress of 3.7 GPa of CN<sub>x</sub> coatings are obtained at –400 V 200 W, whereas the lowest friction coefficient of 0.12 of CN<sub>x</sub> coatings is achieved at –800 V 100 W. Raman and XPS analysis suggest that sp<sup>3</sup> carbon bonding decreases and sp<sup>2</sup> carbon bonding increases with the variations in substrate bias voltage and target sputtering power. Optical images and Raman characterization of worn surfaces confirm that the friction behavior of CN<sub>x</sub> coatings is controlled by the directly sliding between CN<sub>x</sub> coating and steel pin. Therefore, the reduction of friction coefficient is attributed to the decrease of sp<sup>3</sup> carbon bonding in the CN<sub>x</sub> coating. It is concluded that substrate bias voltage and target sputtering power are effective parameters for tailoring the structural and tribological properties of CN<sub>x</sub> coatings.

© 2014 Elsevier B.V. All rights reserved.

## 1. Introduction

Excellent performances of carbon nitride (CN<sub>x</sub>) coatings, such as low friction and high wear resistance make them good candidates for the demanding mechanical systems [1,2]. Particularly, CN<sub>x</sub> coatings produced by the ion beam assisted deposition (IBAD)

\* Corresponding author. Institute of Nanosurface Science and Engineering, College of Mechatronics and Control Engineering, Shenzhen University, Shenzhen 518060, China. Tel.: +86 755 26656730.

E-mail address: [wangpf@szu.edu.cn](mailto:wangpf@szu.edu.cn) (P. Wang).

technique can give super-low frictions ( $\mu < 0.01$ ) in  $N_2$  gas environment [3–6]. According to previous research, the structural and tribological properties of  $CN_x$  coatings are strongly related to the coating deposition methods [3,4,7–10]. However, the key deposition parameter in controlling the tribological behavior as well as structural behavior of  $CN_x$  coatings is still not clearly identified. To obtain a clear relationship among deposition parameter, tribological behavior, and structural behavior of  $CN_x$  coatings, a unique hybrid coating process [11–14], combining radio frequency plasma enhanced chemical vapor deposition (RF PECVD) and DC magnetron sputtering and possessing the advantage of separately adjusting the various deposition parameters (e.g. pressure, source gases, RF power, substrate bias voltage, target materials, and DC sputtering power) have been applied for the development of high performance  $CN_x$  coatings in our recent work [15]. It has been clarified that the structural properties (i.e. deposition rate, residual stress, and hardness) of hybrid  $CN_x$  coatings are greatly affected by the  $N_2/Ar$  flow ratio in the coating process. However, the friction behavior of hybrid  $CN_x$  coatings in  $N_2$  gas stream shows less dependency on the  $N_2/Ar$  flow ratio. The friction coefficients of hybrid  $CN_x$  coatings sliding against AISI 52100 pins in  $N_2$  gas stream are in the ranges of 0.33–0.42, at least 10 times higher than those observed in IBAD  $CN_x$  coatings. Low friction coefficient of hybrid  $CN_x$  coatings is not achieved, although the atomic composition of the hybrid  $CN_x$  coating (81.4% C, 10.8% N, and 7.8% O) is similar to that of the IBAD  $CN_x$  coating (81.8% C, 11.2% N, and 7.0% O). Therefore, it is argued that the bonding structure other than the composition of  $CN_x$  coating is paramount important for achieving low frictions of  $CN_x$  coatings in  $N_2$  gas environment [15].

The structural properties of  $CN_x$  coatings can be tailored by the nitrogen ion energy in the plasma during the coating deposition process [16–19]. It has been revealed that both N/C atomic ratio and  $sp^3/sp^2$  carbon ratio of IBAD  $CN_x$  coatings decrease with increasing bombarding energy of nitrogen ions from 300 eV to 1000 eV [19]. On the other hand, the nitrogen ion energy in the hybrid coating process could be well controlled by adjusting the substrate bias voltage and target sputtering power. Therefore, in this study, effects of substrate bias voltage and target sputtering power on the structural and tribological properties of hybrid  $CN_x$  coatings are investigated, with the objective to get lower friction coefficient of the hybrid  $CN_x$  coatings and further clarify the friction mechanisms of hybrid  $CN_x$  coatings from the viewpoint of bonding structure as well.

## 2. Experimental

### 2.1. Coating deposition

$CN_x$  coatings (400 nm thick) were grown on Si (100) substrates using a hybrid coating process with the combination of RF PECVD and DC magnetron co-sputtering of a graphite target [11–15]. A high purity graphite target (>99.99%) with dimensions of  $\phi 76.2 \times 5$  mm was mounted on the water cooled cathode at a distance of 100 mm from the substrate. A stainless steel shutter was placed between the target and substrate. The base pressure of depositing chamber was pumped down to  $4.0 \times 10^{-4}$  Pa by utilizing a turbomolecular pumping system. First of all, the silicon substrates were etched by argon plasma for 10 min to remove contamination. Thereafter, the shutter was closed and argon plasma was generated on the surface of the graphite target by applying 200 W d.c. power to pre-sputter the target and stabilize the sputtering condition at the surface. The shutter was then opened and  $CN_x$  coatings were deposited onto the silicon substrates at a pressure of 1.3 Pa. A mixture of nitrogen and argon gas with  $N_2/Ar$  flow ratio of 0.1 was

applied as source gas. The detailed deposition conditions are listed in Table 1.

To get higher nitrogen ion energy during the coating deposition process as much as possible, four combinations of substrate bias voltage and target sputtering power in the order of –400 V 200 W, –400 V 100 W, –800 V 200 W, and –800 V 100 W, were employed. The substrate bias voltage increased from –400 V to –800 V, whereas the target sputtering power decreased from 200 W to 100 W. In the hybrid coating process, –800 V was the maximum value of substrate bias voltage, beyond which the re-sputtering rate of the coating by nitrogen and argon ions was larger than the deposition rate of coating, and thus the coating cannot be prepared on the substrate. 200 W was the maximum value of sputtering power, beyond which a strong reaction between nitrogen gas and carbon atom occurred, the reaction product then covered the surface of graphite target and prohibited the deposition process (so-called target poison).

### 2.2. Coating characterization

A surface profiler (Alpha-Step 500 KLA-Tencor Ltd., USA) was employed for thickness and residual stress measurement. The deposition rate was calculated from the thickness of coating, which was determined from a step between the  $CN_x$  coating and silicon substrate generated by a shadow mask. Another purpose to use the surface profiler is to calculate the residual stress of the coating. The residual stress was calculated from the Stoney equation after the measurement of the curvature of  $CN_x$  coated substrate [15,20].

Hardness of  $CN_x$  coatings was evaluated under both single stiffness mode and continuous stiffness mode for confirmation of the results. In case of the single stiffness mode, the hardness of  $CN_x$  coatings was characterized on a Nano Indentation tester (ENT-2100, Elionix Inc., Japan) using a Berkovich diamond tip with a load of 0.4 mN. The depth of indentation was below 10% of the coating thickness in order to exclude the influence of substrate. In case of the continuous stiffness mode, the hardness of  $CN_x$  coatings was determined on a Nano Indenter (Nano Indenter XP, MTS Systems Corporation, USA) using a Berkovich diamond tip with a load of 50 mN. Before and after each experimental series, the tip shape calibration procedure was repeated by indenting a standard fused silica specimen to monitor the possible wear of tip shape. In both conditions, the measurement was conducted ten times on each sample to ensure data accuracy.

Chemical composition and bonding structures of  $CN_x$  coatings were characterized by an X-ray photoelectron spectroscope (XPS, PHI1600, Physical Electronics Inc., USA) operating with a monochromated Mg  $K\alpha$  irradiation. The structure of carbon bonds of  $CN_x$  coatings was analyzed by a Raman spectroscope (NRS-5100, JASCO Corporation, Japan) operating with a 532 nm green laser as the excitation source. The fitting of XPS and Raman spectra were both conducted in Origin 8.0 software (OriginLab Corporation, USA).

Tribological properties of  $CN_x$  coatings were measured by using a pin-on-plate reciprocating tribometer.  $CN_x$  coated Si substrates ( $10 \times 20$  mm) were driven to run against AISI 52100 balls ( $\phi = 6$  mm) with a normal load of 1 N, a sliding speed of  $3 \text{ mm s}^{-1}$ , a

**Table 1**  
Deposition conditions of  $CN_x$  coatings.

Deposition parameters	Value
Operation pressure (Pa)	1.3
$N_2$ gas flow rate (ccm)	1.0
Ar gas flow rate (ccm)	10.0
Substrate bias voltage (V)	–400, –800
Target sputtering power (W)	100, 200

**Table 2**  
The deposition rate, N/C atomic ratio, residual stress, and friction coefficient of CN<sub>x</sub> coatings.

Deposition condition	Deposition rate (nm min <sup>-1</sup> )	N/C atomic ratio	Residual stress (GPa)	Hardness (GPa)	Friction coefficient in N <sub>2</sub> gas stream
-400 V 200 W	6.0	0.15	3.7	15.0	0.33
-400 V 100 W	3.1	0.14	3.9	14.9	0.23
-800 V 200 W	4.8	0.10	4.2	13.0	0.16
-800 V 100 W	1.6	0.10	4.4	12.4	0.12

stroke length of 3 mm, and a sliding period of 5000 cycles. Friction tests were performed in N<sub>2</sub> gas stream in order to exclude the effect of reactive species in air (water vapor and oxygen molecules) on the friction behavior of CN<sub>x</sub> coatings. N<sub>2</sub> gas was blown to the contact interface by a gas nozzle (inner diameter of 4.5 mm) with a flow rate of 2.0 L min<sup>-1</sup>. The worn surfaces on the pins were observed with an optical microscope. The structural changes of those worn surfaces were detected by Raman spectroscopy.

### 3. Results and discussion

#### 3.1. Composition and structure of CN<sub>x</sub> coatings

Deposition rate, N/C atomic ratio and residual stress of CN<sub>x</sub> coatings are summarized in Table 2. Specifically, the deposition rate of CN<sub>x</sub> coatings decreased greatly with the increase of substrate bias voltage from -400 to -800 V as well as the decrease of target sputtering power from 200 to 100 W. The lowest deposition rate of 1.6 nm min<sup>-1</sup> was obtained at substrate bias voltage of -800 V and target sputtering power of 100 W (denoted as -800 V 100 W), which was approximately one-fourth of the deposition rate at -400 V 200 W. The N/C atomic ratio of CN<sub>x</sub> coatings decreased from 0.15 to 0.10 with the increase of substrate bias voltage from -400 to -800 V, whereas it kept almost constant with decreasing target sputtering power from 200 W to 100 W. The residual stress increased slightly with the increase of substrate bias voltage and the decrease of target sputtering power. The lowest residual stress of 3.7 GPa was observed at -400 V 200 W.

According to the deposition mechanism of CN<sub>x</sub> coating using the hybrid coating process, carbon atom is sputtered from the graphite target by a mixture of nitrogen and argon ions, and nitrogen atom is incorporated into the carbon coating from the active nitrogen species in the plasma. On the one hand, the decrease of target sputtering power caused a reduction in the sputter yield of carbon atom from the graphite target, and thus the deposition rate decreased greatly with the decrease of target sputtering power. At the same time, the decrease of target sputtering power resulted in a reduction in the amount of nitrogen ions irradiated onto the carbon coatings due to the decrease in plasma density. Therefore, the N/C atomic ratio of the coatings can hardly be modified by the target sputtering power. The residual stress of CN<sub>x</sub> coatings, which was strongly related to the N/C atomic ratio, was slightly changed with the decrease of target sputtering power [15,21]. On the other hand, the increase of substrate bias voltage led to an increase in the bombardment energy of nitrogen and argon ions arriving at substrate. Re-sputtering of the growing coating by the high-energy nitrogen and argon ions occurred, resulting in lower deposition rate [22,23]. The sputtering rate of nitrogen atom in CN<sub>x</sub> coating is much higher than that of carbon atom [22,23]. The preferential sputtering of nitrogen atom should be responsible for the reduction of N/C atomic ratio at higher substrate bias voltage. The decrease in N/C atomic ratio caused an increased residual stress, which is in consistent with our previous research [15].

As the sputtering yield of carbon atoms was scarcely affected by the substrate bias voltage, the decrease in deposition rate

by substrate bias voltage was less than that by target sputtering power. However, the bombardment energy of nitrogen ions increased greatly by increasing substrate bias voltage, thus the N/C atomic ratio and corresponding residual stress were affected greater by the substrate bias voltage than those by the target sputtering power.

Bonding structures of carbon and nitrogen atoms in CN<sub>x</sub> coatings were characterized by Raman spectroscopy and XPS, respectively. The Raman spectra and typical fitting curves of CN<sub>x</sub> coatings are shown in Fig. 1. The Raman spectrum was profile-fitted with a Lorentzian function for D peak located around 1350 cm<sup>-1</sup>, a Breit–Wigner–Fano (BWF) function for G peak located around 1550 cm<sup>-1</sup>, and a linear function for background subtraction [24–29]. The fitting results for Raman spectra are shown in Table 3. Two representative parameters, peak intensity ratio of D peak and G peak ( $I(D)/I(G)$ ) and coupling coefficient ( $Q$ ) were employed for clarifying the bonding states of carbon atoms. According to past research, the peak intensity ratio ( $I(D)/I(G)$ ) is related to the volume fraction of sp<sup>3</sup> carbon bonding, the increase in peak intensity ratio indicates a decrease in volume fraction of sp<sup>3</sup> carbon bonding [25–27]. The coupling coefficient ( $Q$ ) is correlated to the volume fraction of sp<sup>2</sup> carbon bonding; the increase in coupling coefficient means an increase in volume fraction of sp<sup>2</sup> carbon bonding [24,26,28]. In the current work, the  $I(D)/I(G)$  increased from 1.7 to 2.1 and the  $Q$  increased from -4.8 to -3.2 with the increase of substrate bias voltage and the decrease of target sputtering power, suggesting that sp<sup>3</sup> carbon bonding decreases and sp<sup>2</sup> carbon bonding increases with the variations in substrate bias voltage and target sputtering power. These results agree well with the previous studies, where the amount of sp<sup>2</sup>/sp<sup>3</sup> carbon ratio increases with the increase of bombardment energy of nitrogen ions in the deposition process [17,19,28].

A typical N1s core level spectrum of CN<sub>x</sub> coating prepared under -800 V 100 W is shown in Fig. 2. This spectrum was profile-fitted with Gaussian-shaped lines. The deconvoluted N1s spectrum showed three peaks at 398.3 eV, 399.5 eV, and 399.6 eV, which

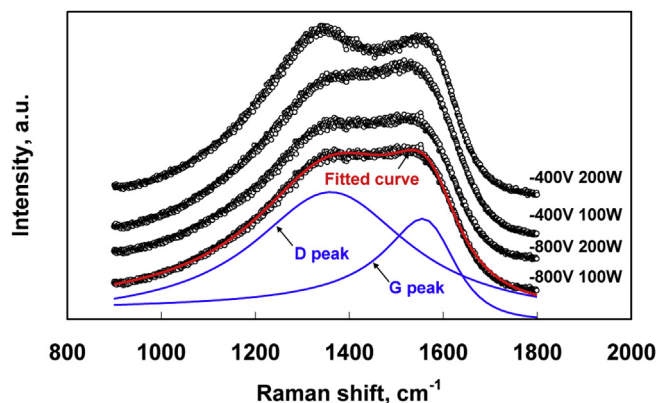


**Fig. 1.** Raman spectra of CN<sub>x</sub> coatings and typical profile-fitting of Raman spectrum of CN<sub>x</sub> coatings prepared at -800 V 100 W.

**Table 3**The fitting results for Raman and XPS spectra of CN<sub>x</sub> coatings.

Deposition condition	D peak (cm <sup>-1</sup> )	G peak (cm <sup>-1</sup> )	I(D)/I(G)	Q	N1s sp <sup>2</sup> C=N/sp <sup>3</sup> C–N
–400 V 200 W	1338	1581	1.7	–4.8	1.5
–400 V 100 W	1362	1580	1.6	–3.9	2.5
–800 V 200 W	1360	1580	1.8	–3.8	2.4
–800 V 100 W	1360	1581	2.1	–3.2	2.3

were attributed to sp<sup>3</sup> C–N, sp<sup>2</sup> C=N, and N–O bonds, respectively [15,27,30–33]. The variation of sp<sup>2</sup> C=N/sp<sup>3</sup> C–N ratio of N1s peak with substrate bias voltage and target sputtering power is provided in Table 3. The sp<sup>2</sup> C=N/sp<sup>3</sup> C–N ratio increased greatly from 1.5 to 2.5 with the decrease of target sputtering power from 200 W to 100 W. With the further changes in substrate bias voltage and target sputtering power, the sp<sup>2</sup> C=N/sp<sup>3</sup> C–N ratio kept almost constant (2.5–2.3). In summary of the Raman and XPS analysis, it was concluded that sp<sup>3</sup> carbon bonding decreases and sp<sup>2</sup> carbon bonding increases with the changes in substrate bias voltage and target sputtering power.

### 3.2. Hardness of CN<sub>x</sub> coatings

Hardness curves of CN<sub>x</sub> coatings measured by single and continuous stiffness modes are shown in Fig. 3(a) and (b), respectively. In case of the single stiffness mode, a specific hardness value at peak load of 0.4 mN was obtained. As summarized in Table 2, the hardness of CN<sub>x</sub> coatings decreased from 15.0 to 12.4 GPa with the increase of substrate bias voltage and the decrease of target sputtering power. The highest hardness of 15.0 GPa was obtained at 200 W –400 V.

In case of the continuous stiffness mode, a curve of hardness in relation to the plastic penetration depth is shown in Fig. 3(b). The typical hardness of the coating was obtained from the peak value of the curve. Therefore, it was clarified that the hardness of CN<sub>x</sub> coatings decreases in the following order: –400 V 200 W > –400 V 100 W > –800 V 200 W > –800 V 100 W. The decreasing tendency of hardness with the penetration depth, which can clearly be observed from the curve of –400 V 100 W, was due to the substrate effect [34]. Since the measured hardness is more or less influenced by the substrate, the comparison of relative hardness among hybrid CN<sub>x</sub> coatings is more significant than the exact value for the current study [19,35]. Consequently, it was concluded that the hardness of CN<sub>x</sub> coatings decreases with the increase of substrate bias voltage and the decrease of target sputtering power.

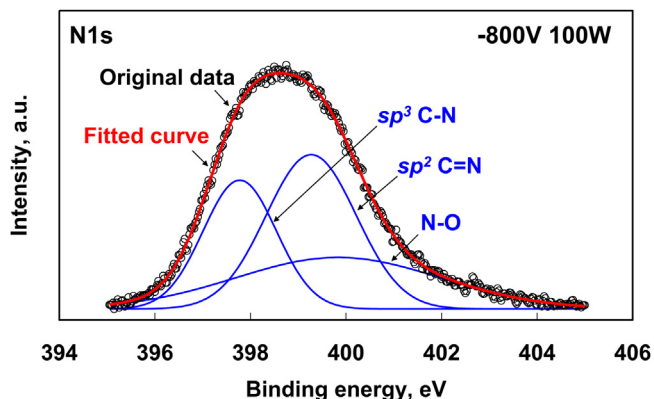


Fig. 2. Typical N1s core level spectrum of CN<sub>x</sub> coating prepared at –800 V 100 W and corresponding Gaussian curves.

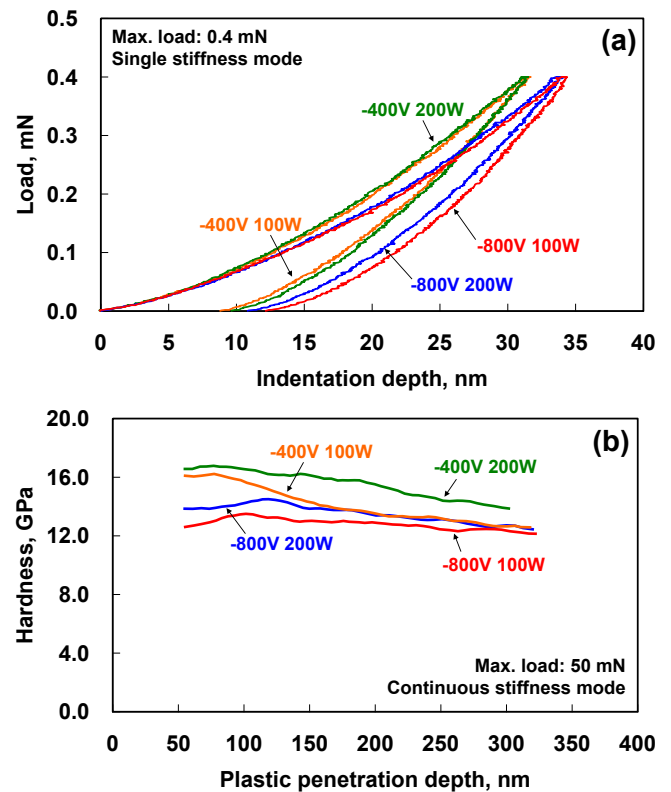


Fig. 3. Hardness curves of CN<sub>x</sub> coatings measured under (a) single stiffness mode and (b) continuous stiffness mode.

The hardness of CN<sub>x</sub> coatings depends strongly on compositions, bonding states and local structures [19,34,35]. It has been argued that the hardness of CN<sub>x</sub> coatings is mainly determined by the volume fraction of sp<sup>3</sup> carbon bonding (sp<sup>3</sup> C–C and sp<sup>3</sup> C–N) in the coating [22,36,37]. According to the Raman and XPS analysis results, the decrease in sp<sup>3</sup> carbon bonding causes the decreased hardness of CN<sub>x</sub> coating in this study.

### 3.3. Tribological behavior of CN<sub>x</sub> coatings

Friction curves of CN<sub>x</sub> coatings sliding against AISI 52100 pins in N<sub>2</sub> gas stream are shown in Fig. 4. The friction values in N<sub>2</sub> gas stream reached steady state after 2000 cycles. The average friction coefficients of CN<sub>x</sub> coatings in N<sub>2</sub> gas stream, which were calculated from the final 1000 cycles in the friction test, are summarized in

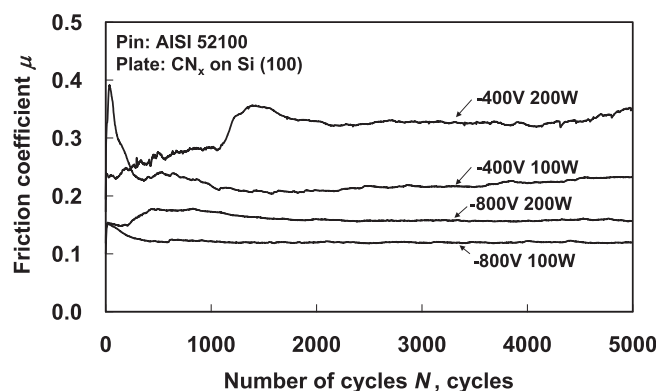


Fig. 4. Friction curves of CN<sub>x</sub> coatings sliding against AISI 52100 pins in N<sub>2</sub> gas stream.

**Table 2.** The average friction coefficients decreased with increasing substrate bias voltage and decreasing target sputtering power. The friction coefficient decreased in the subsequent order:  $-400\text{ V } 200\text{ W} > -400\text{ V } 100\text{ W} > -800\text{ V } 200\text{ W} > -800\text{ V } 100\text{ W}$ , which is in the same tendency to that of hardness. The lowest friction coefficient of 0.12 of  $\text{CN}_x$  coatings in  $\text{N}_2$  gas stream was obtained at  $-800\text{ V } 100\text{ W}$ .

It was found that higher substrate bias voltage and lower target sputtering power are beneficial for reducing the friction coefficients of  $\text{CN}_x$  coatings in  $\text{N}_2$  gas stream. According to the deposition mechanism, the increase of substrate bias voltage and decrease of target sputtering power caused a relative increase in nitrogen ion energy. Therefore, it was clarified that the increase of nitrogen ion energy in this research is effective in reducing friction coefficients of  $\text{CN}_x$  coatings in  $\text{N}_2$  gas stream. To clarify the mechanism for the reduced friction coefficient, the worn surfaces were analyzed by optical microscopy and Raman spectroscopy.

Optical images of worn surfaces on the AISI 52100 pins after friction tests in  $\text{N}_2$  gas stream are shown in Fig. 5. Tribo-film was clearly observed on the worn surface of pin. The amount of tribo-film on the pin surface decreased gradually from Fig. 5(a)–(d) with the changes in substrate bias voltage and target sputtering power. In particular, very few amount of tribo-film was observed on the worn surface of pin after sliding against  $\text{CN}_x$  coating produced at  $-800\text{ V } 100\text{ W}$ .

The formation of tribo-film on the pin surface is closely related to the tribochemical reactions between the amorphous carbon and iron in the  $\text{CN}_x$  coating and steel pin, respectively. It is believed that by removing the iron oxide on the top surface of the steel pin during the initial sliding process (so-called running-in), strong reactions between carbon and iron occur, resulting in the build-up of tribo-film on the steel pin surface [38]. As can be seen in Fig. 5, it was assumed that the increase of the hardness of  $\text{CN}_x$  coatings increases the abrasive wear on the pin surface. Consequently, the severe scratch and removal of the iron oxide on the pin surface leading to stronger reactions on the contact interface and thus higher amount of tribo-film on the pin surface. As the hardness of

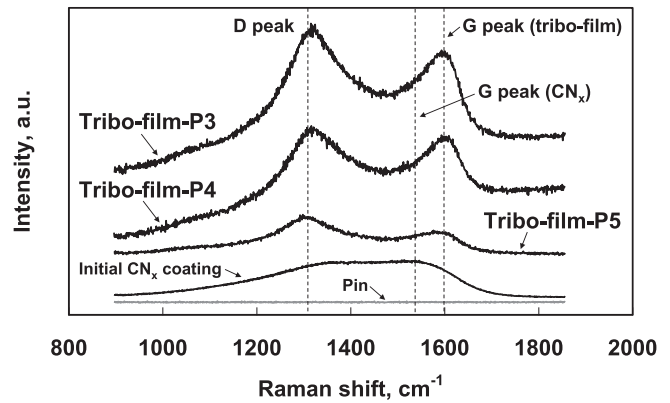


**Fig. 6.** Typical Raman spectra of tribo-films on the AISI 52100 pin surfaces after sliding against  $\text{CN}_x$  coatings in  $\text{N}_2$  gas stream. The spectra of initial  $\text{CN}_x$  coating and AISI 52100 pin are also shown for reference.

$\text{CN}_x$  coatings prepared under  $-800\text{ V } 100\text{ W}$  (12.4 GPa) is more closed to that of iron oxide [13,38,39], the iron oxide on the steel pin surface is hardly removed. Moreover, reaction of the carbon is more favorable with iron than with iron oxide. Therefore, few amount of tribo-films were observed on the steel pin surface, as shown in Fig. 5(d).

Raman spectra of tribo-films on the worn surfaces of pins are shown in Fig. 6. The Raman spectra of P1 and P2 in Fig. 5(a) can be found in our previous work [15]. The appearance of D peak and G peak together with the shift of G peak to a higher wavenumber on the Raman spectrum suggested the formation of a graphite-like structure in the tribo-film. The graphite-like structure is necessary for achieving low friction coefficients of less than 0.10 of carbon-based coatings in  $\text{N}_2$  gas environment [2,5,6,33,40]. However, this graphite-like structure is not enough for obtaining low friction coefficients of hybrid  $\text{CN}_x$  coatings in  $\text{N}_2$  gas environment. It has been proposed in our recent research that the high friction coefficients between 0.33 and 0.42 in  $\text{N}_2$  gas stream are due to

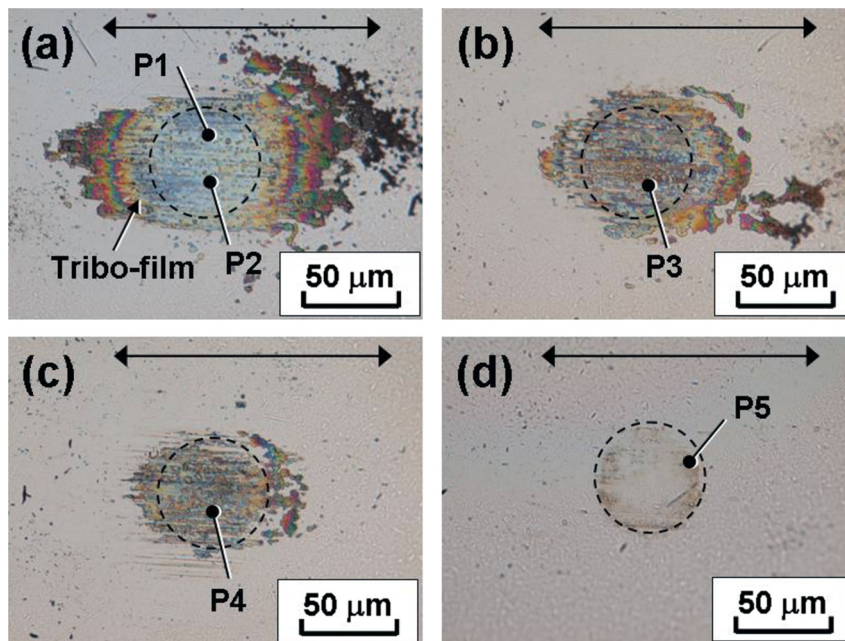


**Fig. 5.** Optical images of worn surfaces on the AISI 52100 pins after sliding against  $\text{CN}_x$  coatings prepared at (a)  $-400\text{ V } 200\text{ W}$ , (b)  $-400\text{ V } 100\text{ W}$ , (c)  $-800\text{ V } 200\text{ W}$ , and (d)  $-800\text{ V } 100\text{ W}$ . The black arrows indicate the sliding direction of the pin. The dotted circles indicate the theoretical contact area on the steel pin surface.

directly sliding between  $CN_x$  coating and steel pin surface [15]. With the changes in substrate bias voltage and target sputtering power, graphite-like structure was still observed on the tribo-film from the Raman analysis, as shown in Fig. 6. However, it is still not the key point for the friction reduction, as the amount of tribo-film on the ball surface decreased with the decrease in friction coefficient. Especially, the lowest friction coefficient was obtained with very few amounts of tribo-films on the ball surface, as shown in Fig. 5(d). Additionally, the Raman spectra of worn surfaces on the  $CN_x$  coated silicon plates (not shown here) are identical to that of the initial  $CN_x$  coating (as shown in Fig. 6), which suggests that structural changes are not occurred on the worn surfaces of the plate. Therefore, it was argued that the friction behavior of hybrid  $CN_x$  coating is still controlled by the directly sliding between  $CN_x$  coating and steel pin surface, the decrease of friction coefficient is attributed to the structural changes of  $CN_x$  coatings.

The role of carbon bonding in the friction mechanism of carbon-based coating has been extensively investigated in the former research. In case of a steel ball sliding against diamond-like carbon (DLC) coating, it has been argued that reaction between  $sp^3$  C–R bond (R is macro-radicals) and steel ball leads to strong adhesive force and causes high friction [41]. From the molecular dynamics simulation result, it has been argued that preventing the formation of  $sp^3$  C–C bond results in the low and stable friction coefficient of IBA  $CN_x$  coating in  $N_2$  gas environment [42]. Thus, the decrease of  $sp^3$  carbon bonding in the hybrid  $CN_x$  coatings is beneficial for reducing the friction coefficient in  $N_2$  gas stream. Furthermore, it has been clarified that the decrease in the friction coefficients of  $CN_x$  coatings prepared by magnetron sputtering can be correlated to the contribution of the  $sp^2$  C=N bond in the coating structure [43].  $CN_x$  coatings having the highest  $sp^2$  C=N/ $sp^2$  C=C ratio give the best tribological performance (lowest friction coefficient of 0.14 and lowest specific wear rate of  $27.5 \times 10^{-7} \text{ mm}^3 \text{ Nm}^{-1}$ ) in  $N_2$  gas environment. Therefore, it was claimed that the decrease of  $sp^3$  carbon bonding and the increase of  $sp^2$  carbon bonding in the hybrid  $CN_x$  coatings reduce the adhesive force between the  $sp^3$  carbon bonding and carbon tribo-film formed on the steel pin surface, thus resulting in the reduced friction coefficient in  $N_2$  gas stream.

According to the structural changes in hybrid  $CN_x$  coatings with the variation of  $N_2/Ar$  flow ratio [15], substrate bias voltage, and target sputtering power, it has been clarified that  $sp^2$  C=N/ $sp^3$  C–N ratio decreases with the increase of  $N_2/Ar$  flow ratio and the minimum value is 0.7, whereas the  $sp^2$  C=N/ $sp^3$  C–N increases with the increase of substrate bias voltage and the decrease of target sputtering power and the maximum value is 2.5. On the other hand, the friction coefficients of  $CN_x$  coatings sliding against AISI 52100 pins in  $N_2$  gas stream keep almost constant with the increase in  $N_2/Ar$  flow ratio, but the friction coefficients decrease greatly with the increase of substrate bias voltage and the decrease of target sputtering power. Therefore, a close relationship between the amount of  $sp^2$  C=N bonding and friction behavior of the hybrid  $CN_x$  coatings in  $N_2$  gas stream was confirmed. It was strongly argued that higher amount of  $sp^2$  C=N compared with that of  $sp^3$  C–N in the hybrid  $CN_x$  coatings definitely minimize the adhesion force between steel pin surface and hybrid  $CN_x$  coating, thus leading to low frictions of hybrid  $CN_x$  coatings in  $N_2$  gas stream.

It has been clarified that increase of  $sp^2$  C=N/ $sp^3$  C–N is favorable for reducing the friction coefficients of  $CN_x$  coatings in  $N_2$  gas stream. Therefore, it can be summarized that substrate bias voltage and target sputtering power are more effective than  $N_2/Ar$  flow ratio for preparing hybrid  $CN_x$  coatings with low friction performance, which suggest that control of nitrogen ion energy in the coating process is an effective pathway for obtaining  $CN_x$  coatings with outstanding mechanical and tribological

performances. Moreover, the increase of nitrogen ion energy facilitates the formation of  $sp^2$  C=N bonds in the  $CN_x$  coatings and the detailed mechanisms will be clarified in our future work.

#### 4. Summary

Effects of substrate bias voltage and target sputtering power on the structural and tribological properties of  $CN_x$  coatings prepared by a hybrid coating process with the combination of RF PECVD and DC magnetron sputtering have been investigated in this study. The main results are concluded as follows.

- (1) With the increase of substrate bias voltage and the decrease of target sputtering power in the order of  $-400 \text{ V } 200 \text{ W}$ ,  $-400 \text{ V } 100 \text{ W}$ ,  $-800 \text{ V } 200 \text{ W}$ , and  $-800 \text{ V } 100 \text{ W}$ , the deposition rate decreases from 6.0 to  $1.6 \text{ nm min}^{-1}$ , N/C atomic ratio decreases from 0.15 to 0.10, and hardness of  $CN_x$  coatings measured under single stiffness mode decreases from 15.0 to 12.4 GPa, whereas the residual stress of  $CN_x$  coatings increases from 3.7 to 4.4 GPa. The highest hardness of 15.0 GPa and the lowest residual stress of 3.7 GPa of  $CN_x$  coatings are obtained at  $-400 \text{ V } 200 \text{ W}$ .
- (2) Friction coefficients of  $CN_x$  coatings sliding against AISI 52100 pins in  $N_2$  gas stream decrease greatly from 0.33 to 0.12 with the increase of substrate bias voltage and the decrease of target sputtering power. The lowest friction coefficient of 0.12 of  $CN_x$  coatings in  $N_2$  gas stream is achieved at  $-800 \text{ V } 100 \text{ W}$ .
- (3) It is clarified that  $sp^3$  carbon bonding decreases and  $sp^2$  carbon bonding increases with the increase of substrate bias voltage and the decrease of target sputtering power. The reduction of friction coefficient is attributed to the decrease of  $sp^3$  carbon bonding in the  $CN_x$  coating.

#### Acknowledgments

This work was partly supported by the Grant-in-Aid for Scientific Research (A) (23246038) and (B) (22360043) of the Japan Society for the Promotion of Science (JSPS), the Taiho Kogyo Tribology Research Foundation, and the Global COE Program, “World Center of Education and Research for Trans-disciplinary Flow Dynamics”, Ministry of Education, Culture, Sports, Science and Technology (MEXT) in Japan. This research was also performed by the JSPS Core-to-Core Program “International research core on smart layered materials and structures for energy saving”. We would like to acknowledge them for their financial support.

#### References

- [1] J.C. Sánchez-López, A. Fernández, in: C. Donnet, A. Erdemir (Eds.), *Tribology of Diamond-like Carbon Films*, Springer, New York, 2008, p. 311.
- [2] K. Adachi, K. Kato, in: C. Donnet, A. Erdemir (Eds.), *Tribology of Diamond-like Carbon Films*, Springer, New York, 2008, p. 339.
- [3] J.C. Sánchez-López, M. Belin, C. Donnet, C. Quirós, E. Elizalde, *Surf. Coat. Technol.* 160 (2002) 138.
- [4] K. Kato, N. Umehara, K. Adachi, *Wear* 254 (2003) 1062.
- [5] P. Wang, K. Adachi, *Tribol. Online* 6 (2011) 265.
- [6] P. Wang, M. Hirose, Y. Suzuki, K. Adachi, *Surf. Coat. Technol.* 221 (2013) 163.
- [7] C. Morant, L.A. Fernández, C. Quirós, G.G. Fuentes, E. Elizalde, J.M. Sanz, *Surf. Interface Anal.* 30 (2000) 638.
- [8] Y. Kusano, Z.H. Barber, J.E. Evetts, I.M. Hutchings, *Surf. Coat. Technol.* 124 (2000) 104.
- [9] C. Jama, A. Al khawwam, A.-S. Loir, P. Goudmand, O. Dessaux, L. Gengembre, J. Grimblot, *Surf. Interface Anal.* 31 (2001) 815.
- [10] A.A. Voevodin, J.G. Jones, T.C. Back, J.S. Zabinski, V.E. Strel'nitzki, I.I. Aksenov, *Surf. Coat. Technol.* 197 (2005) 116.
- [11] H. Miki, T. Takeno, T. Takagi, *Thin Solid Films* 516 (2008) 5414.
- [12] T. Takeno, H. Miki, T. Sugawara, Y. Hoshi, T. Takagi, *Diamond Relat. Mater.* 17 (2008) 713.

- [13] H. Miki, K. Ito, T. Sugawara, J. Fontaine, T. Takeno, M. Ruet, M. Belin, K. Adachi, T. Takagi, *Tribol. Online* 4 (2009) 60.
- [14] T. Takeno, S. Abe, K. Adachi, H. Miki, T. Takagi, *Diamond Relat. Mater.* 19 (2010) 548.
- [15] P. Wang, T. Takeno, K. Adachi, H. Miki, T. Takagi, *Appl. Surf. Sci.* 258 (2012) 6576.
- [16] I. Bertóti, A. Tóth, M. Mohai, T. Ujvári, *Surf. Interface Anal.* 30 (2000) 538.
- [17] Y.H. Cheng, B.K. Tay, S.P. Lau, X. Shi, X.L. Qiao, Z.H. Sun, J.G. Chen, Y.P. Wu, C.S. Xie, *Diamond Relat. Mater.* 10 (2001) 2137.
- [18] S. Wei, T. Shao, P. Ding, *Diamond Relat. Mater.* 19 (2010) 648.
- [19] S. Wei, T. Shao, J. Xu, *Surf. Coat. Technol.* 206 (2012) 3944.
- [20] G.G. Stoney, *Proc. R. Soc. Lond. A* 82 (1909) 172.
- [21] D.F. Franceschini, C.A. Achete, F.L. Freire Jr., *Appl. Phys. Lett.* 60 (1992) 3229.
- [22] Y. Togashi, Y. Hirohata, T. Hino, *Vacuum* 66 (2002) 391.
- [23] H. Ling, J.D. Wu, J. Sun, W. Shi, Z.F. Ying, N. Xu, W.J. Pan, X.M. Ding, Z.Y. Zhou, *Diamond Relat. Mater.* 11 (2002) 1584.
- [24] S. Praver, K.W. Nugent, Y. Lifshitz, G.D. Lempert, E. Grossman, J. Kulik, I. Avigal, R. Kalish, *Diamond Relat. Mater.* 5 (1996) 433.
- [25] J. Robertson, *Mater. Sci. Eng. Rep.* 37 (2002) 129.
- [26] T. Takeno, H. Miki, T. Takagi, H. Onodera, *Diamond Relat. Mater.* 15 (2006) 1902.
- [27] F. Zhou, K. Adachi, K. Kato, *Thin Solid Films* 514 (2006) 231.
- [28] L. Han, X. Chen, L. Yang, Y. Wang, X. Wang, Y. Zhao, *Appl. Surf. Sci.* 257 (2011) 6945.
- [29] S. Yamamoto, A. Kawana, H. Ichimura, C. Masuda, *Surf. Coat. Technol.* 210 (2012) 1.
- [30] X. Yan, T. Xu, G. Chen, S. Yang, H. Liu, Q. Xue, *J. Phys. D: Appl. Phys.* 37 (2004) 907.
- [31] T.W. Scharf, R.D. Ott, D. Yang, J.A. Barnard, *J. Appl. Phys.* 85 (1999) 3142.
- [32] Z. Wang, C. Wang, Q. Wang, J. Zhang, *J. Appl. Phys.* 104 (2008) 073306.
- [33] T. Tokoroyama, M. Kamiya, N. Umehara, C. Wang, D. Diao, *Lubr. Sci.* 24 (2012) 129.
- [34] P. Papakonstantinou, P. Lemoine, *J. Phys.: Condens. Matter* 13 (2001) 2971.
- [35] S. Wei, T. Shao, *Mater. Chem. Phys.* 135 (2012) 733.
- [36] X.C. Wang, Z.Q. Li, P. Wu, E.Y. Jiang, H.L. Bai, *Diamond Relat. Mater.* 15 (2006) 1732.
- [37] X. Jiang, C. Zhuang, J. Zhao, X. Jiang, *Diamond Relat. Mater.* 23 (2012) 44.
- [38] J. Fontaine, T. Le Mogne, J.L. Loubet, M. Belin, *Thin Solid Films* 482 (2005) 99.
- [39] S. Takaki, K. Kawasaki, Y. Kimura, *J. Mater. Process. Technol.* 117 (2001) 359.
- [40] Y. Liu, A. Erdemir, E.I. Meletis, *Surf. Coat. Technol.* 82 (1996) 48.
- [41] H. Li, T. Xu, C. Wang, J. Chen, H. Zhou, H. Liu, *Diamond Relat. Mater.* 15 (2006) 1228.
- [42] K. Tezuka, Master Thesis, Tohoku University, Japan, 2010, p. 99 (in Japanese).
- [43] J.C. Sánchez-López, C. Donnet, M. Belin, T. Le Mogne, C. Fernández-Ramos, M.J. Sayagués, A. Fernández, *Surf. Coat. Technol.* 133–134 (2000) 430.